HHS Public Access

Author manuscript

Oncogene. Author manuscript; available in PMC 2021 May 16.

Published in final edited form as:

Oncogene. 2021 January ; 40(3): 578–591. doi:10.1038/s41388-020-01550-2.

HDAC6 promotes growth, migration/invasion and self-renewal of rhabdomyosarcoma

Thao Q. Pham[1,*], **Kristin Robinson**[1,*], **Lin Xu**[2,3], **Maria N. Pavlova**[1], **Stephen X. Skapek**[2], **Eleanor Y. Chen**[1,**]

[1]Department of Laboratory Medicine and Pathology, University of Washington, Seattle, WA

[2]Department of Pediatrics, Department of Population & Data Sciences, University of Texas Southwestern Medical Center, Dallas, TX

[3]Quantitative Biomedical Research Center, Department of Population & Data Sciences, University of Texas Southwestern Medical Center, Dallas, TX

Abstract

Rhabdomyosarcoma (RMS) is a devastating pediatric sarcoma. The survival outcomes remain poor for patients with relapsed or metastatic disease. Effective targeted therapy is lacking due to our limited knowledge of the underlying cellular and molecular mechanisms leading to disease progression. In this study, we used functional assays *in vitro* and *in vivo* (zebrafish and xenograft mouse models) to demonstrate the crucial role of HDAC6, a cytoplasmic histone deacetylase, in driving RMS tumor growth, self-renewal and migration/invasion. Treatment with HDAC6-selective inhibitors recapitulates the HDAC6 loss-of-function phenotypes. HDAC6 regulates cytoskeletal dynamics to promote tumor cell migration and invasion. RAC1, a Rho family GTPase, is an essential mediator of HDAC6 function, and is necessary and sufficient for RMS cell migration and invasion. High expression of RAC1 correlates with poor clinical prognosis in RMS patients. Targeting the HDAC6-RAC1 axis represents a promising therapeutic option for improving survival outcomes of RMS patients.

Keywords

rhabdomyosarcoma; invasion; migration; metastasis; self-renewal; HDAC6; RAC1

**Corresponding author Contact information: eleanor2@uw.edu, phone: 206-616-5062.
*Equal contribution to the manuscript.

AUTHOR CONTRIBUTIONS

EYC contributes to designing and performing the experiments, data analysis and writing the manuscript. TP, KR and MP contribute to performing the experiments and data analysis. LX and SS contribute to data analysis.

CONFLICT OF INTEREST STATEMENT

The authors have no conflict of interest to declare.

INTRODUCTION

Rhabdomyosarcoma (RMS) is a devastating pediatric sarcoma that displays morphological and molecular evidence for incomplete myogenic differentiation. RMS is roughly divided into two major subtypes by histologic features, embryonal (ERMS) and alveolar (ARMS). Genetically, ERMS is characterized by mutations in the receptor tyrosine kinase/RAS/PIK3CA axis found in at least 90% of cases (1), and most ARMS cases harbor the PAX3 (or PAX7)-FOXO1 fusion transcript (2). Despite the genetic differences, the prognosis for relapsed or metastatic disease remains poor regardless of the subtype. Effective targeted therapy is lacking due to our poor understanding of events leading to relapse or metastasis of RMS.

Several studies have shed some light on some of the genes and pathways that contribute to the metastatic potential of RMS. For example, Hepatocyte Growth Factor (HGF) and Stromal-derived Factor −1 (SDF-1) regulate metastatic behavior of cMet-positive RMS cells by directing them to the lymph nodes and the bone marrow (3), and downregulation of the MET-CXCR4 axis decreases the migration of RMS cells in response to the SDF-1 or HGF gradients *in vitro* (4). Deficiency of tp53 in a conserved zebrafish model of ERMS increases the metastatic potential of ERMS cells (5). Additional targets involved in the signaling pathways such as IL-4R and Plexin-A1 have also been shown to promote migratory and metastatic capacity of RMS cells (6,7). However, the cellular and molecular mechanisms leading to invasion and metastasis of RMS cells remain to be elucidated. Specifically, the molecular players involved in altering the cytoskeletal dynamics to orchestrate RMS tumor cell invasion and metastasis remain to be identified and characterized.

Cancer stemness is mainly characterized by the self-renewal capacity of cancer cells to give rise to progeny cells that recapitulate the cancer heterogeneity (8). The therapeutic potential of targeting cancer stem cells in solid tumors (e.g. skin squamous cell carcinoma, colorectal cancer and non-small cell lung cancer) has been demonstrated in a variety of pre-clinical animal models (9–11). The inhibitors against several pathways involved in regulating the maintenance and survival of cancer stem cells (e.g. the Wnt, Notch and Hedgehog pathways) are in various phases of clinical trials (12,13). However, the insight into the genes and pathways that regulate the stemness of RMS remains limited. Molecular markers such as myf5, a marker for activated muscle satellite cells, and CD133, a transmembrane glycoprotein, have been used to enrich for tumor propagating cells in pre-clinical models of RMS (14,15). Canonical and non-canonical Wnt pathways and TP53 have been shown to modulate the self-renewal capacity of RMS tumor-propagating cells (5,16,17). Further investigation in preclinical models is necessary to identify additional druggable targets against the cancer stemness of RMS and determine the therapeutic benefit of targeting cancer stemness in RMS.

In our previous CRISPR screen of the Histone Deacetylases (HDACs), HDAC6 is among the selected HDACs that are essential for RMS tumor cell growth (18). Unlike the other HDACs, HDAC6 predominantly exerts its function in the cytoplasm and has been shown to interact with substrates such as Heat Shock Protein 90 (HSP90), Extracellular signal-related Kinase 1 (ERK1), KRAS, Tubulin and Cortactin to regulate diverse cellular processes such

as cell migration, adhesion and growth in several normal and neoplastic cell types (19–23). HDAC6 has been shown to either promote or suppress cancer cell invasion and metastasis depending on the cancer cell type (24,25). Besides the studies on the role of HDAC6 in regulating the maintenance of glioma stem cells (26,27), there is limited knowledge on the function of HDAC6 in regulating self-renewal capacity of cancer cells.

In this study, we investigate the function of HDAC6 in various RMS features utilizing both *in vitro* and *in vivo* functional assays and demonstrate that HDAC6 is essential for RMS cell growth, migration/invasion and self-renewal. RAC1, a Rho GTPase, is a key player in mediating HDAC6 function in regulating RMS cell migration/invasion. High expression of RAC1 correlates with poor clinical survival of RMS patients. Overall, targeting the HDAC6-RAC1 axis may have significant therapeutic benefits for RMS patients.

RESULTS

Expression of HDAC6 in RMS

We assessed expression of HDAC6 in primary human RMS samples by immunohistochemistry. HDAC6 expression was detected primarily in the cytoplasm at variable intensity levels in most cases of ARMS (11 of 11) and ERMS (6 of 7) (Fig. 1 A–F). In contrast, five cases of pediatric muscle did not express HDAC6 (Fig. 1F). A panel of ERMS (RD and SMS-CTR) and ARMS cell lines (Rh5 and Rh30) showed cytoplasmic and perinuclear expression of HDAC6 by immunofluorescence (Fig. 1 G–J). Overall, our findings showed that HDAC6 is differentially expressed in RMS cells compared to muscle, and that HDAC6 localizes predominantly in the cytoplasm of RMS cells.

Conserved role of HDAC6 in promoting tumor growth in RMS

To assess HDAC6 loss-of-function effects tumor cell growth, we generated CRISPR/Cas9-mediated *HDAC6* gene knockout using two gRNAs targeting exons 5 and 8 (Fig. 1 K) by lentivral transduction in a panel of RMS cell lines (ERMS: RD, 381T, SMS-CTR; ARMS: Rh5 and Rh30). Targeted disruption of *HDAC6* resulted in a significant reduction of tumor cell growth 5 days post-plating (Fig. 1 L). To assess the specificity of *HDAC6* knockout on tumor cell growth, we performed rescue experiments in a stable RD cell line harboring tamoxifen-inducible Cas9 and the same set of HDAC6 gRNAs (Fig. 1 K) by overexpressing Green Fluorescent Protein (GFP) as a control, wild-type HDAC6 and catalytically-dead (cd) HDAC6 (both modified to be Cas9-resistant) in RD cells harboring tamoxifen-inducible CRISPR/Cas9 targeting *HDAC6*. The two histidine-to-alanine mutations (H216A and H611A) inactivate the deacetylase activity of HDAC6 (23). Overexpression of Cas9-resistant, wild-type HDAC6 alleviated the *HDAC6* knockout-induced growth phenotype in comparison with overexpression of Cas9-resistant cd HDAC6 or GFP 6 days post-tamoxifen induction (Fig. 1 M). Similarly, overexpression of Cas9-resistant wild-type HDAC6 also rescued the growth phenotype in Rh5 cells with *HDAC6* knockout (Fig. S1 A). Overexpressing HDAC6 alone did not affect RMS tumor cell growth significantly (Fig. S1 B). Our findings indicate that the effect of *HDAC6* knockout on tumor cell growth is specific and that the catalytic activity of HDAC6 is required for its function in regulating RMS tumor cell growth. Depletion of HDAC6 protein from CRISPR/Cas9-mediated gene knockout in

lentivirus-transduced and tamoxifen-inducible lines as well as overexpression of wild-type and cd HDAC6 were confirmed by Western blots (Fig. 1 N).

To assess the effects of HDAC6 loss-of-function on tumor growth *in vivo*, we generated CRISPR/Cas9-mediated *hdac6* knockout in a zebrafish model of KRAS(G12D)-induced ERMS (28). Double gRNAs targeting exons 5 and 10 of *hdac6* generated an approximately a 5-kb deletion in 7 of 8 randomly selected *hdac6*-targeted zebrafish tumors (Fig. S1 C), indicating high targeting efficiency. ERMS tumors expressed *hdac6* (Fig. S1 D), and depletion of *hdac6* mRNA to approximately 40–50% relative to scrambled control gRNA-injected tumors was observed in 7 of 8 randomly selected *hdac6*-targeted zebrafish tumors (Fig. S1 E). Zebrafish ERMS tumors harboring *hdac6* knockout (n = 8) showed significantly reduced tumor growth by at least 50% compared to tumors harboring the GFP-scrambled control gRNAs (n = 10) (Fig. 1 O–S). In addition, targeted disruption of *hdac6* did not alter tumor onset but increased overall tumor-free survival in zebrafish (Fig. S1 F). Our findings indicate that Hdac6 has a conserved role in promoting ERMS tumor growth and progression.

HDAC6 promotes RMS tumor growth by modulating cell cycle progression and tumor cell differentiation

To determine the tumor cell phenotypes that contributed to reduced tumor cell growth following targeted disruption of *HDAC6*, we assessed for alterations in cell cycle progression, cell death and cell differentiation in stable RD and Rh5 lines harboring the tamoxifen-inducible Cas9/*HDAC6* double gRNA cassette. RD and Rh5 cells with tamoxifen-induced *HDAC6* knockout showed altered progression in G1 or G2/M phases of cell cycle day 6 post-tamoxifen induction (Fig. 2 A) but no significant change in programmed cell death at the same time point (Fig. 2 B). RMS cells show abnormal arrest in myogenic differentiation (16,18). We have previously shown that CRISPR-mediated *HDAC6* disruption resulted in a modest increase in myogenic differentiation of 381T ERMS cells (18). Here we observed that on immunofluorescence staining for myosin heavy chain (MF20), targeted disruption of *HDAC6* also resulted in a modest increase in myogenic differentiation of the RD ERMS line (approximately 1.5–2 fold; $p < 0.01$) compared to no tamoxifen-treated controls following 72-hour starvation in 2% horse serum starting at day 4 post-tamoxifen treatment (Fig. 2 C–E). There was a slightly larger increase in the percentage of MF20-positive cells in tamoxifen-treated Rh5 cells (approximately 2–3 folds increase) compared to the no tamoxifen-treated controls; $p < 0.01$) (Fig. 2 C, F–G). RD and Rh5 cells harboring targeted *HDAC6* also showed variable increase in the expression levels of genes involved in myogenesis (e.g. *MYOD1*, *MYH8*, *CKM*) at distinct time points following targeted disruption of *HDAC6*, (Fig. 2 H–I) Based on our findings, HDAC6 promotes RMS tumor growth in part by modulating cell cycle progression and tumor cell differentiation.

HDAC6 promotes RMS tumor cell migration and self-renewal

The effects of HDAC6 loss-of-function on the migratory behavior and self-renewal capacity of RMS cells were also assessed in RD and Rh5 lines carrying the tamoxifen-inducible Cas9/*HDAC*6 double gRNA cassette. Following 3 days of tamoxifen-induced *HDAC6* targeting, RD and Rh5 were plated for corresponding assays. RD and Rh5 cells with targeted disruption of *HDAC6* showed reduced gap closure at 16 hours post-scratch in scratch wound

healing assays (Fig. 3 A–B) as well as reduced transwell migration towards the chemoattractant (fetal bovine serum) 22 hours post-seeding in the top chamber (Fig. 3 C–D).

Using the sphere assay as a surrogate *in vitro* assay for assessing tumor cell stemness and self-renewal (29), we showed that RD and Rh5 cells with tamoxifen-induced CRISPR/Cas9-mediated *HDAC6* gene disruption exhibited reduced frequency and size of sphere formation following 3 days of culturing in stem cell medium and low-attachment condition (Fig. 3 E–F). A previous study demonstrates that spheres generated from the RD line show upregulated expression of stem cell markers such as *NANOG*, *SOX2* and *OCT4* (14). Here we showed that expression levels of *SOX2*, *NANOG* and OCT4 were reduced in RD sphere cells with tamoxifen-induced *HDAC6* knockout (Fig. 3 G). Overexpression of Cas9-resistant wild-type HDAC6 rescued the expression of these stem cell markers (Fig. 3 G).

Overall, our findings using *in vitro* functional assays suggest that HDAC6 plays an important role in regulating migratory and self-renewal capacity of RMS tumor cells.

HDAC6 alters the cytoskeletal dynamics to affect RMS cell migration via RAC1

HDAC6 has previously been shown to acetylate the elements of cytoskeleton such as tubulin and actin (20,30). To assess whether HDAC6 plays a role in modulating the dynamics of cytoskeleton to promote migration of RMS tumor cells, we showed that there were increased levels of acetylated tubulin in RD and Rh5 cells following targeted disruption of *HDAC6* by CRISPR/Cas9 (Fig. 4 A). Overexpressing wild-type but not catalytically-dead (cd) Cas9-resistant HDAC6 in RD cells harboring targeted disruption of *HDAC6* alleviated the migratory defect in comparison to overexpressing GFP as a control (Fig. 4 B; Fig. S2 A), indicating that the deacetylase activity is required for the HDAC6 function in regulating RMS cell migration. To assess the effects of HDAC6 loss-of-function on actin-dependent cytoskeletal dynamics, we showed by phalloidin staining that there was loss of membrane ruffles, folds and filopodia as well as altered organization of cytoplasmic actin filament in RD and Rh5 cells with targeted disruption of *HDAC6* following Epidermal Growth Factor (EGF) stimulation in the setting of serum starvation (Fig. 4 C; Fig. S2 B).

RAC1 is a small GTPase of the Rho family which has been shown to mediate a variety of cellular events including cell adhesion, motility and polarity (31,32). However, the causal relationship between HDAC6 and RAC1 in mediating the cytoskeletal dynamics to promote RMS cell migration is unclear. To assess whether RAC1 contributes to HDAC6-mediated changes in the cytoskeleton dynamics and cell motility of RMS cells, we first showed that RAC1 and HDAC6 co-localized in the regions of cell membrane ruffles and folds (Fig. 4 D; Fig. S2 C), and that RAC1-GTP levels were reduced in RMS cells with *HDAC6* knockout (Fig. 4 E). Overexpressing the constitutively activated mutant form of RAC1 (RAC1V12) alleviated the migration phenotype (Fig. 4 F) but did not significantly alter the growth phenotype of RD cells with *HDAC6* knockout (Fig. 4 G). A dominant-negative form of RAC1 (RAC1N17) and a constitutively active form of mutant RhoA (RhoAV14), another Rho family GTPase, did not rescue the migration defect or the growth defect in RMS cells with *HDAC6* knockout (Fig. 4 F–G). Using a RAC1-GTP pull-down assay, RAC1V12 immunoprecipitated increased level of RAC1-GTP compared to GFP control and RAC1N17, supporting the constitutive activity of RAC1V12 (Fig. 4 H). Taken together, HDAC6 alters

the microtubule and actin-dependent cytoskeletal dynamics to promote RMS cell migration via RAC1, and there is no cross talk between close members of Rho GTPases in this context.

RAC1 is essential for RMS cell migration and invasion

As RAC1 is a key mediator of HDAC6 function in regulating RMS cell migration, we next assessed whether RAC1 is essential for RMS cell migration and invasion through loss-of-function and gain-of-function studies. Cultured RD and Rh5 cells with CRISPR/Cas9-mediated targeted disruption of *RAC1* showed reduced migratory capacity by the scratch wound healing assay (16 hours post-scratch, $p < 0.0001$; Fig. 5 A–B; Fig. S2 D). Overexpression of Cas9-resistant RAC1V12 rescued the loss-of-function effects of RAC1 on cell migration, indicating the specificity of the CRISPR/Cas9-mediated *RAC1* targeting (Fig. 5 C). Targeted disruption of *RAC1* had mild effect (approximately 10–15% reduction) on RD cell growth and no significant effect on Rh5 cell growth (7 days post-plating, $p < 0.0001$; Fig. 5 D). Finally, RD and Rh5 cells treated with the selective RAC1 inhibitor, EHop-016, also showed reduced migration (Figure S2 E).

To assess the gain-of-function effects of RAC1 on RMS cell growth and invasion *in vivo*, KRASG12D-driven zebrafish ERMS tumors co-expressing Green Fluorescent Protein (GFP) and RAC1V12 or empty vector as a control were sorted for green fluorescence-positive cells and transplanted into syngeneic CG1 zebrafish at 10,000 cell per fish via dorsal subcutaneous route. The fish with engrafted tumors were imaged weekly and harvested after 21 days. RAC1V12-expressing tumors ($n = 12$) showed larger increase in tumor volume over 1-week period compared to control tumors ($n = 9$) (Fig. 5 E–F; Fig. S2 F). By 21 days, zebrafish ERMS tumor cells co-expressing RAC1V12 demonstrate more aggressive growth compared to the control empty vector co-expressing tumor cells (Fig. 5 E). On histologic analysis, RAC1V12 co-expressing zebrafish ERMS tumors are deeply invasive into the skeletal muscle compared to control empty vector co-expressing zebrafish ERMS tumors, which showed only superficial invasion in about the same period (Fig. 5 G).

RAC1 is associated with poor prognosis in RMS

To assess whether *HDAC6* or *RAC1* expression is associated with clinical prognosis in RMS, we correlated expression levels of *HDAC6* or *RAC1* mRNA expression in 81 cases with survival data (63 fusion-negative and 18 fusion-positive). Kaplan-Meier curves were generated based on gene expression values dichotomized into over- and under-expressed groups combining fusion-negative and fusion-positive patients using the median expression value within each cohort as a cutoff. While expression of *HDAC6* did not correlate with overall survival, high expression of *RAC1* correlated with decreased overall survival (Fig. 5 H log rank test, $p = 0.02842$, HR = 2.36, 95% CI = 1.095 – 5.084). If we stratify the analysis by fusion status, RAC1 expression showed marginal significance for the fusion-negative ($p= 0.07036$) but not the fusion-positive cases ($p=0.31$) with respect to overall survival. Although the small sample size in both subsets compromises the ability to draw firm conclusions, the findings suggest that expression of *RAC1* might be useful as a clinical prognostic biomarker if they are confirmed in a prospective analysis.

Treatment with HDAC6-selective inhibitors recapitulates the HDAC6 loss-of-function effects in RMS

To assess whether treatment of RMS cells with selective HDAC6 inhibitors, tubastatin A and tubacin, could recapitulate the loss-of-function effects of HDAC6 on RMS cells, we first showed that treating a panel of RMS cell lines (RD, SMS-CTR, Rh5 and Rh30) with tubastatin A and tubacin *in vitro* significantly inhibited tumor cell growth in a dose-dependent manner (Fig. 6 A; Fig. S3 A). RD and Rh5 cells treated with tubastatin A and tubacin showed increased levels of acetylated tubulin, a known substrate of HDAC6 (30) (Fig. 6 B; Fig. S3 B). In scratch wound healing assays, RD and Rh5 were treated tubastatin A (200 nM) or tubacin (500 nM) for 24 hours prior to plating and kept under treatment throughout each assay. Tubastatin A or tubacin-treated RD and Rh5 cells showed reduced gap closure at 16 hours (Fig. 6 C–D; Fig. S3 C). RD and Rh5 cells treated with tubastatin A (200 nM) or tubacin (500 nM) for 3 days also showed reduced sphere formation (Fig. 6 E–F; Fig. S3 D).

To assess the effect of tubastatin A treatment on RMS tumor growth *in vivo*, RMS xenografts generated from RD and Rh5 cells were treated with tubastatin A by intraperitoneal injections at 10 mg per kg per mouse every 3 days for 21 days. RD and Rh5 xenografts harvested at the end of the treatment period showed increased expression of acetylated tubulin by immunohistochemistry (Fig. S4 A–H), indicating that treatment of tubastatin A selectively inhibited HDAC6 activity *in vivo*. RMS xenografts treated with tubastatin A showed at least 50% reduction in tumor growth compared to those treated with DMSO as a vehicle control (Fig. 6 G–H; Fig. S4 I–J). RMS xenograft tumors treated with tubastatin A also showed reduced Ki67 proliferation index based on immunohistochemistry analysis (Fig. S4 K–L).

To assess whether tubastatin A treatment affects the self-renewal capacity of RMS cells *in vivo*, we treated 20–21 days-old ERMS tumor-bearing zebrafish with tubastatin A (10 μM) and DMSO (vehicle) for 7 days and performed limiting dilution transplantation assays. A time course analysis showed that zebrafish tumors treated with 10 μM of tubastatin showed increased levels of acetylated tubulin as early as 24 to 48 hours post-treatment compared to ones treated with vehicle control (DMSO), indicating selective targeting of HDAC6 activity in zebrafish ERMS tumors (Fig. S4 M). Tumor engraftment was monitored weekly until day 30 post-transplantation. In 3 independent experiments, tubastatin A-treated ERMS tumors transplanted at limiting dilutions (10^4, 10^3 and 10^2 cells) showed approximately 6–9 fold decrease in self-renewal frequency by Extreme Limiting Dilution (ELDA) analysis (33) (Table 1). Overall, treatment of RMS cells with tubastatin A and tubacin mimics the loss-of-function effects of HDAC6 on tumor cell growth, migration and self-renewal capacity and represents promising agents of targeted therapy for RMS.

DISCUSSION

HDAC6 has been shown to deacetylate tubulin, a subunit of microtubule, and cortactin, an actin-associated protein, to affect cytoskeletal dynamics (20,30). A study in mouse embryonic fibroblasts demonstrates that functional HDAC6 is required for RAC1 activation (23). However, the functional relationship among HDAC6, the microtubule and the actin

filament in driving cancer cell invasion/migration is unclear. In our study, we showed that HDAC6 deacetylates the tubulin subunits of microtubule, and its deacetylase activity is required to promote RMS cell migration. HDAC6 also plays a crucial role in regulating the actin-dependent cytoskeletal dynamics required for RMS cell migration. This is supported by our findings that HDAC6 and RAC1 co-localize in the areas of membrane ruffles and filopodia, which are the changes in the actin elements required for cell motility and invasion, and RMS cells with targeted disruption of *HDAC6* showed reduced formation of membrane ruffling and filopodia. In addition, RAC1 has been shown previously to be required for actin polymerization, stress fiber formation and focal adhesion complex assembly (31). In this study, loss of HDAC6 resulted in reduced RAC1 GTPase activity, and activated mutant form of RAC1 (RAC1V12) alleviated the migration defect of RMS cells with *HDAC6* knockout. Overall, our findings indicate that the deacetylate activity of HDAC6 and activation of RAC1 are essential for the HDAC6-mediated effects on actin-dependent cytoskeletal dynamics required for RMS cell migration and invasion. The crosstalk between the microtubules and actin elements in regulating cellular processes such as cell migration is beginning to be recognized (34). HDAC6 likely coordinates the direct or indirect interactions between the microtubules and the actin or its associated molecules to promote RMS cell migration and invasion. Further investigation is required to assess whether acetylation of tubulin or other substrates by HDAC6 directly affects RAC1 activation and in turn actin dynamics or HDAC6 independently alters the microtubule and actin dynamics to regulate RMS cell motility.

RAC1 is required for actin cytoskeletal reorganization, a process required for cell migration/invasion during cancer metastasis. Increased expression or activity of RAC1 is associated with metastatic potential in multiple cancer types (e.g. breast, liver and upper urinary tract) (35–37). In this study, we used loss-of-function and gain-of-function studies *in vitro* and *in vivo* to demonstrate that RAC1 is necessary and sufficient for active migration/invasion of RMS cells. Further investigation will be required to assess whether RAC1 is required to initiate metastasis of RMS cells.

Our analysis of clinical data showed that the expression levels of *HDAC6* do not correlate with overall survival of RMS patients, suggesting that HDAC6 might be involved in a complex gene interaction network, and that epistatic interactions may mask the effect of HDAC6 on overall survival. By contrast, high expression of *RAC1* correlates with poor overall survival in RMS patients. Additional analyses with larger data sets are needed to confirm the possible prognostic value of RAC1 expression within each subgroup (fusion-positive vs fusion-negative), and multivariate analyses are needed to evaluate whether its expression is independent of tumor stage or clinical risk groups already established to correlate with outcome for children with RMS. Beyond this, our findings indicate that HDAC6 and RAC1 can serve as therapeutic targets for reducing invasive and metastatic potential of RMS cells.

The self-renewal capacity of tumor initiating cells contributes to cancer relapse and therapy resistance (12). So far there are limited studies on characterizing the role of HDAC6 in regulating cancer stemness and self-renewal capacity. In glioblastoma, HDAC6 is required for maintaining the glioma stem cell stemness and contributes through its interaction with

the Sonic Hedgehog (SHH) signaling pathway to promote the radio-resistant phenotype (26). Through *in vitro* sphere assays, stem cell marker analysis and *in vivo* limiting dilution assays, we showed that CRISPR/Cas9-mediated targeted disruption of *HDAC6* and treatment with a selective HDAC6 inhibitor, tubastatin A or tubacin, resulted in reduced cancer stemness and self-renewal capacity of RMS cells. RMS spheres generated *in vitro* have been shown to be enriched for stem cell markers and are resistant to treatment with standard-of-care chemotherapy agents (14). While further investigation is required to determine the pathways modulated by HDAC6 to regulate self-renewal of RMS cells, our findings suggest that targeted therapy using HDAC6 selective inhibitors against cancer stemness represents a promising option for preventing relapse and treatment resistance in RMS.

Our knowledge in the molecular mechanisms underlying RMS self-renewal and metastasis is limited. Using *in vitro* and *in vivo* functional assays, we have characterized the unique role of HDAC6 in regulating RMS tumor growth, self-renewal and migration/invasion. As RAC1 serves as an essential downstream mediator of HDAC6 function in RMS cell migration and invasion, targeting the HDAC6-RAC1 axis will likely improve survival outcomes of RMS patients.

METHODS

CRISPR/Cas9 Gene Targeting in Human RMS Cell Lines

Single knockout was accomplished by transducing RMS cells with lentiviral virus expressing safe-harbor control or gene-specific double gRNAs (Table S1) and Cas9. Cells transduced with lentivirus were plated for cell-based assays following antibiotic selection 5 days post-transduction. Cloning of Cas9 and gRNA expression vectors was performed as described previously (18).

CRISPR/Cas9 inducible cells were created using piggybac transposition (1). Stable cell lines were integrated with a construct containing double gRNAs and ERT-Cas9-ERT fusion protein for tamoxifen inducible gene targeting. The coding portions of wild-type and cd *HDAC6* were amplified from the plasmids (38) obtained from Addgene (Watertown, MA) for cloning purposes. Lentiviral RAC1V12 and RHOAN17 expression constructs were obtained from the Langenau lab (17). Silent mutations to alter PAM sites to create Cas9-resistant wild-type HDAC6, cd HDAC6 and RAC1V12 lentiviral overexpression constructs used in rescue and overexpression experiments were introduced using a 4-piece Gibson cloning strategy. All cell lines were previously authenticated by STR profiling and tested for mycoplasma contamination.

Assessing Tumor Growth and Self-renewal Using Zebrafish ERMS Model

Zebrafish were maintained in a shared facility at the University of Washington under protocol #4330–01 approved by the University of Washington Subcommittee on Research Animal Care. The *rag2*:*KRAS(G12D)*-U6:*hdac6* gRNAs construct was made by the Gibson cloning strategy to insert the U6:*hdac6* gRNAs cassette into the *rag2*:KRAS(G12) construct obtained from the Langenau lab (Massachusetts General Hospital/Harvard Medical School).

The *rag2* promoter and Cas9 coding region were inserted into the *rag2*:Cas9 expression construct using the Gibson cloning strategy. To introduce CRISPR/Cas9-mediated gene targeting in the zebrafish model of KRAS-driven ERMS, a cocktail of DNA constructs containing *rag2*:*KRAS(G12)*-U6-*hdac6* gRNAs, *rag2*:Cas9 and *myog*-H2B:RFP was injected into zebrafish embryos at 1-cell stage. Deletion of *hdac6* in zebrafish tumors was confirmed by sequencing the PCR products amplified using the primers flanking the gRNA sites (Table S1). Tumor volume change was assessed as previously described (39). Additional details for tumor volume assessment and limiting dilution assays are in Supplemental Methods.

Cell-based Assays

Cell counts, Cell Titer Glo assay, immunofluorescence for MF20, Annexin V assay, sphere assay and scratch/wound healing assay were performed based on the protocols previously described (18, 39). RAC1 activation assay was performed using the RAC1 Activation Assay Biochem Kit (Cytoskeleton, Inc., Denver, CO). Additional details are in Supplemental Methods.

Human Xenografts and Drug Treatment

Mouse studies were approved by the University of Washington Subcommittee on Research Animal Care under protocol #4330–01. To establish xenografts in immunocompromised NOD-SCID Il2rg−/− (NSG) mice, approximately 1–2 × 10^6 RMS cells (Rh5 or RD) were resuspended in Matrigel and injected subcutaneously into the flanks of each 6–7 weeks-old anesthetized mouse. As tumor size reached approximately 50–100 mm^3, tubastatin-A (10 mg/kg) or vehicle (DMSO) was administered by the intraperitoneal route every 3 days for up to 21 days or until tumor end point (750 mm^3). Tumor size was measured by caliper every 3–4 days at tumor onset until tumor end point or at the end of drug treatment (whichever is earlier).

Survival Association Analysis in RMS patient cohort

The 81 RMS cases with survival and gene expression data were published previously (40). For survival analysis, p value was calculated based on the log-rank test by R package Survival (https://cran.r-project.org/web/packages/survival/index.html). Note that study subject age and sex, available only on a subset of the data, were not incorporated into the survival analyses because those features are not generally accepted as factors that influence survival of RMS patients.

Statistics

Two-tailed t-test and ANOVA tests were used to assess statistical significance in differences between experimental and control samples when appropriate. A p value <0.05 was considered statistically significant.

Additional details for immunohistochemistry, immunofluorescence, Western blots and quantitative RT-PCR are in Supplemental Methods.

Supplementary Material

Refer to Web version on PubMed Central for supplementary material.

ACKNOWLEDGEMENTS

The authors want to thank Terra Vleeshouwer-Neumann and Amy Chen for technical assistance with some experiments. EYC is supported by NIH R01 CA196882. Lin Xu is supported by Children's Cancer Fund and Rally Foundation.

REFERENCES

1. Shern JF, Chen L, Chmielecki J, Wei JS, Patidar R, Rosenberg M, et al. Comprehensive genomic analysis of rhabdomyosarcoma reveals a landscape of alterations affecting a common genetic axis in fusion-positive and fusion-negative tumors. Cancer Discov. 2014 2;4(2):216–31. [PubMed: 24436047]
2. Barr FG, Galili N, Holick J, Biegel JA, Rovera G, Emanuel BS. Rearrangement of the PAX3 paired box gene in the paediatric solid tumour alveolar rhabdomyosarcoma. Nat Genet. 1993 2;3(2):113–7. [PubMed: 8098985]
3. Jankowski K, Kucia M, Wysoczynski M, Reca R, Zhao D, Trzyna E, et al. Both hepatocyte growth factor (HGF) and stromal-derived factor-1 regulate the metastatic behavior of human rhabdomyosarcoma cells, but only HGF enhances their resistance to radiochemotherapy. Cancer Res. 2003 11 15;63(22):7926–35. [PubMed: 14633723]
4. Miekus K, Lukasiewicz E, Jarocha D, Sekula M, Drabik G, Majka M. The decreased metastatic potential of rhabdomyosarcoma cells obtained through MET receptor downregulation and the induction of differentiation. Cell Death Dis. 2013 1 17;4:e459.
5. Ignatius MS, Hayes MN, Moore FE, Tang Q, Garcia SP, Blackburn PR, et al. tp53 deficiency causes a wide tumor spectrum and increases embryonal rhabdomyosarcoma metastasis in zebrafish. Elife. 2018 9 7;7.
6. Hosoyama T, Aslam MI, Abraham J, Prajapati SI, Nishijo K, Michalek JE, et al. IL-4R drives dedifferentiation, mitogenesis, and metastasis in rhabdomyosarcoma. Clin Cancer Res. 2011 5 1;17(9):2757–66. [PubMed: 21536546]
7. Chen EY, Dobrinski KP, Brown KH, Clagg R, Edelman E, Ignatius MS, et al. Cross-species array comparative genomic hybridization identifies novel oncogenic events in zebrafish and human embryonal rhabdomyosarcoma. PLoS Genet. 2013 8;9(8):e1003727.
8. Kreso A, Dick JE. Evolution of the cancer stem cell model. Cell Stem Cell. 2014 3 6;14(3):275–91. [PubMed: 24607403]
9. Chen D, Wu M, Li Y, Chang I, Yuan Q, Ekimyan-Salvo M, et al. Targeting BMI1(+) Cancer Stem Cells Overcomes Chemoresistance and Inhibits Metastases in Squamous Cell Carcinoma. Cell Stem Cell. 2017 5 4;20(5):621–634 e6. [PubMed: 28285905]
10. Hu S, Fu W, Li T, Yuan Q, Wang F, Lv G, et al. Antagonism of EGFR and Notch limits resistance to EGFR inhibitors and radiation by decreasing tumor-initiating cell frequency. Sci Transl Med. 2017 3 8;9(380).
11. Goto N, Fukuda A, Yamaga Y, Yoshikawa T, Maruno T, Maekawa H, et al. Lineage tracing and targeting of IL17RB(+) tuft cell-like human colorectal cancer stem cells. Proc Natl Acad Sci U A. 2019 6 25;116(26):12996–3005.
12. Saygin C, Matei D, Majeti R, Reizes O, Lathia JD. Targeting Cancer Stemness in the Clinic: From Hype to Hope. Cell Stem Cell. 2019 1 3;24(1):25–40. [PubMed: 30595497]
13. Du FY, Zhou QF, Sun WJ, Chen GL. Targeting cancer stem cells in drug discovery: Current state and future perspectives. World J Stem Cells. 2019 7 26;11(7):398–420. [PubMed: 31396368]
14. Walter D, Satheesha S, Albrecht P, Bornhauser BC, D'Alessandro V, Oesch SM, et al. CD133 positive embryonal rhabdomyosarcoma stem-like cell population is enriched in rhabdospheres. PLoS One. 2011;6(5):e19506.

15. Ignatius MS, Chen E, Elpek NM, Fuller AZ, Tenente IM, Clagg R, et al. In vivo imaging of tumor-propagating cells, regional tumor heterogeneity, and dynamic cell movements in embryonal rhabdomyosarcoma. Cancer Cell. 2012 5 15;21(5):680–93. [PubMed: 22624717]
16. Chen EY, DeRan MT, Ignatius MS, Grandinetti KB, Clagg R, McCarthy KM, et al. Glycogen synthase kinase 3 inhibitors induce the canonical WNT/beta-catenin pathway to suppress growth and self-renewal in embryonal rhabdomyosarcoma. Proc Natl Acad Sci U A. 2014 4 8;111(14):5349–54.
17. Hayes MN, McCarthy K, Jin A, Oliveira ML, Iyer S, Garcia SP, et al. Vangl2/RhoA Signaling Pathway Regulates Stem Cell Self-Renewal Programs and Growth in Rhabdomyosarcoma. Cell Stem Cell. 2018 3 1;22(3):414–427 e6. [PubMed: 29499154]
18. Phelps MP, Bailey JN, Vleeshouwer-Neumann T, Chen EY. CRISPR screen identifies the NCOR/HDAC3 complex as a major suppressor of differentiation in rhabdomyosarcoma. Proc Natl Acad Sci U A. 2016 12 12;
19. Tran AD, Marmo TP, Salam AA, Che S, Finkelstein E, Kabarriti R, et al. HDAC6 deacetylation of tubulin modulates dynamics of cellular adhesions. J Cell Sci. 2007 4 15;120(Pt 8):1469–79. [PubMed: 17389687]
20. Zhang X, Yuan Z, Zhang Y, Yong S, Salas-Burgos A, Koomen J, et al. HDAC6 modulates cell motility by altering the acetylation level of cortactin. Mol Cell. 2007 7 20;27(2):197–213. [PubMed: 17643370]
21. Wu JY, Xiang S, Zhang M, Fang B, Huang H, Kwon OK, et al. Histone deacetylase 6 (HDAC6) deacetylates extracellular signal-regulated kinase 1 (ERK1) and thereby stimulates ERK1 activity. J Biol Chem. 2018 2 9;293(6):1976–93. [PubMed: 29259132]
22. Yang MH, Laurent G, Bause AS, Spang R, German N, Haigis MC, et al. HDAC6 and SIRT2 regulate the acetylation state and oncogenic activity of mutant K-RAS. Mol Cancer Res. 2013 9;11(9):1072–7. [PubMed: 23723075]
23. Gao YS, Hubbert CC, Lu J, Lee YS, Lee JY, Yao TP. Histone deacetylase 6 regulates growth factor-induced actin remodeling and endocytosis. Mol Cell Biol. 2007 12;27(24):8637–47. [PubMed: 17938201]
24. Kozyreva VK, McLaughlin SL, Livengood RH, Calkins RA, Kelley LC, Rajulapati A, et al. NEDD9 regulates actin dynamics through cortactin deacetylation in an AURKA/HDAC6-dependent manner. Mol Cancer Res. 2014 5;12(5):681–93. [PubMed: 24574519]
25. Yin Z, Xu W, Xu H, Zheng J, Gu Y. Overexpression of HDAC6 suppresses tumor cell proliferation and metastasis by inhibition of the canonical Wnt/beta-catenin signaling pathway in hepatocellular carcinoma. Oncol Lett. 2018 12;16(6):7082–90. [PubMed: 30546442]
26. Marampon F, Megiorni F, Camero S, Crescioli C, McDowell HP, Sferra R, et al. HDAC4 and HDAC6 sustain DNA double strand break repair and stem-like phenotype by promoting radioresistance in glioblastoma cells. Cancer Lett. 2017 7 1;397:1–11. [PubMed: 28342984]
27. Yang W, Liu Y, Gao R, Yu H, Sun T. HDAC6 inhibition induces glioma stem cells differentiation and enhances cellular radiation sensitivity through the SHH/Gli1 signaling pathway. Cancer Lett. 2018 2 28;415:164–76. [PubMed: 29222038]
28. Langenau DM, Keefe MD, Storer NY, Guyon JR, Kutok JL, Le X, et al. Effects of RAS on the genesis of embryonal rhabdomyosarcoma. Genes Dev. 2007 6 1;21(11):1382–95. [PubMed: 17510286]
29. Pastrana E, Silva-Vargas V, Doetsch F. Eyes wide open: a critical review of sphere-formation as an assay for stem cells. Cell Stem Cell. 2011 5 6;8(5):486–98. [PubMed: 21549325]
30. Hubbert C, Guardiola A, Shao R, Kawaguchi Y, Ito A, Nixon A, et al. HDAC6 is a microtubule-associated deacetylase. Nature. 2002 5 23;417(6887):455–8. [PubMed: 12024216]
31. Guo F, Debidda M, Yang L, Williams DA, Zheng Y. Genetic deletion of Rac1 GTPase reveals its critical role in actin stress fiber formation and focal adhesion complex assembly. J Biol Chem. 2006 7 7;281(27):18652–9. [PubMed: 16698790]
32. Lof-Ohlin ZM, Nyeng P, Bechard ME, Hess K, Bankaitis E, Greiner TU, et al. EGFR signalling controls cellular fate and pancreatic organogenesis by regulating apicobasal polarity. Nat Cell Biol. 2017 11;19(11):1313–25. [PubMed: 29058721]

33. Hu Y, Smyth GK. ELDA: extreme limiting dilution analysis for comparing depleted and enriched populations in stem cell and other assays. J Immunol Methods. 2009 8 15;347(1–2):70–8. [PubMed: 19567251]

34. Dogterom M, Koenderink GH. Actin–microtubule crosstalk in cell biology. Nat Rev Mol Cell Biol. 2019 1;20(1):38–54. [PubMed: 30323238]

35. Zhuang X, Zhang H, Li X, Li X, Cong M, Peng F, et al. Differential effects on lung and bone metastasis of breast cancer by Wnt signalling inhibitor DKK1. Nat Cell Biol. 2017 10;19(10):1274–85. [PubMed: 28892080]

36. Kamai T, Shirataki H, Nakanishi K, Furuya N, Kambara T, Abe H, et al. Increased Rac1 activity and Pak1 overexpression are associated with lymphovascular invasion and lymph node metastasis of upper urinary tract cancer. BMC Cancer. 2010 4 28;10:164. [PubMed: 20426825]

37. Wu L, Cai C, Wang X, Liu M, Li X, Tang H. MicroRNA-142–3p, a new regulator of RAC1, suppresses the migration and invasion of hepatocellular carcinoma cells. FEBS Lett. 2011 5 6;585(9):1322–30. [PubMed: 21482222]

38. Kawaguchi Y, Kovacs JJ, McLaurin A, Vance JM, Ito A, Yao TP. The deacetylase HDAC6 regulates aggresome formation and cell viability in response to misfolded protein stress. Cell. 2003 12 12;115(6):727–38. [PubMed: 14675537]

39. Vleeshouwer-Neumann T, Phelps M, Bammler TK, MacDonald JW, Jenkins I, Chen EY. Histone Deacetylase Inhibitors Antagonize Distinct Pathways to Suppress Tumorigenesis of Embryonal Rhabdomyosarcoma. PLoS One. 2015;10(12):e0144320.

40. Xu L, Zheng Y, Liu J, Rakheja D, Singleterry S, Laetsch TW, et al. Integrative Bayesian Analysis Identifies Rhabdomyosarcoma Disease Genes. Cell Rep. 2018 7 3;24(1):238–51. [PubMed: 29972784]

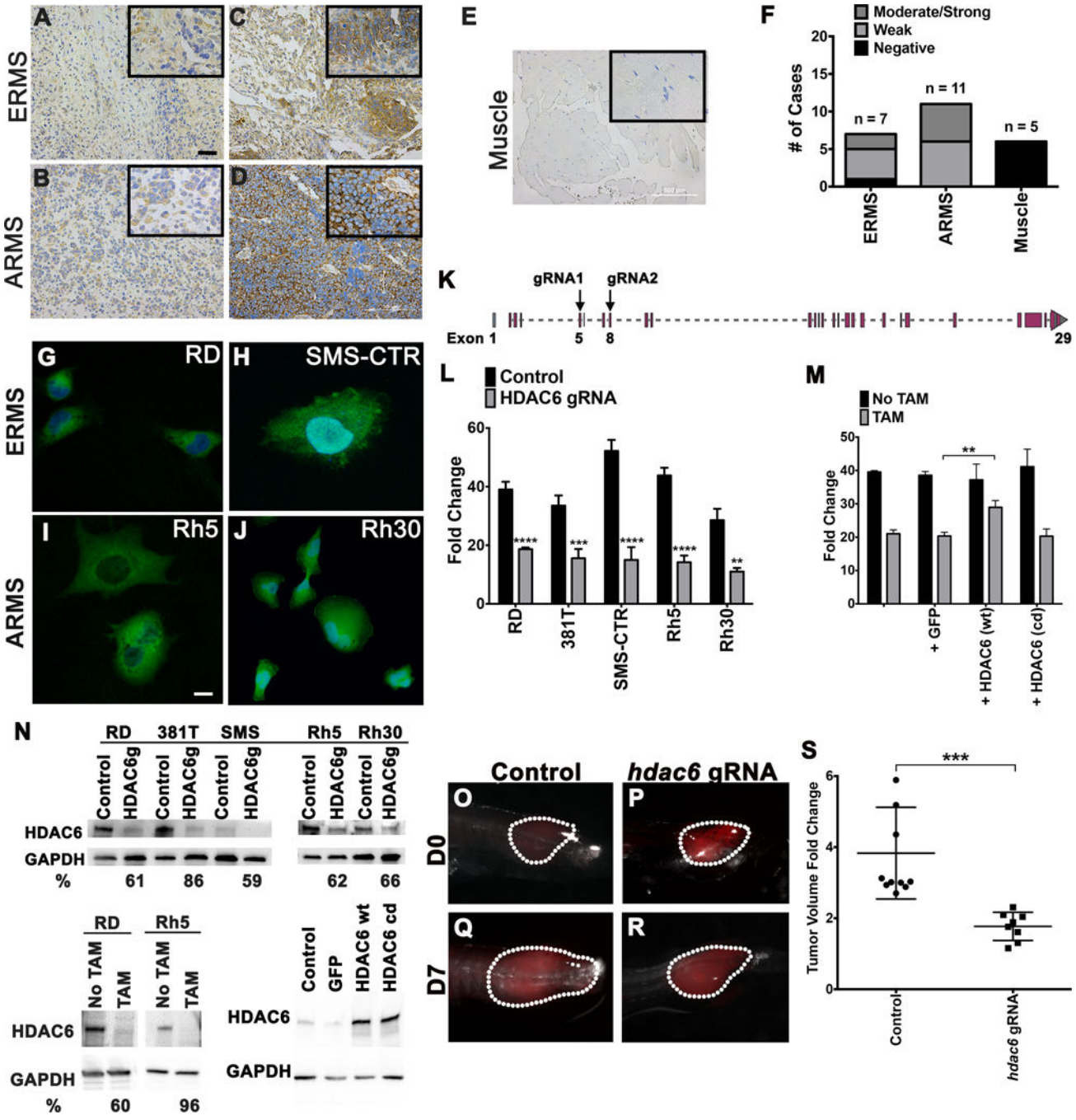

Figure 1. HDAC6 expression in RMS and conserved function of HDAC6 in regulating RMS tumor growth.

(A-E) Immunohistochemistry for HDAC6 in representative primary ERMS and ARMS tumors and skeletal muscle tissue. Weaker staining in (A-B) and stronger staining in (C-D). No staining in skeletal muscle (E). Scale bar = 100 μm. Inset (outlined by bold rectangle) shows a higher-magnification view. (F) Summary of IHC results in ERMS (n = 7), ARMS (n = 11) and skeletal muscle (n = 5) from human patients. (G-J) Immunofluorescense for HDAC6 in (G-H) ERMS cell lines (RD and SMS-CTR) and (I and J) ARMS cell lines (Rh5 and Rh30). (K) A schematic of *hdac6* gRNA locations (exons 5 and 8) used for CRISPR-

mediated gene targeting by lentivirus or tamoxifen-inducible system. (L) Summary of changes in cell growth by cell counts following transduction with lentivirus expressing Cas9 and double *HDAC6* gRNAs for gene knockout (KO) in a panel of RMS cell lines. The results shown are as fold change in cell counts 5 days post-plating and represent the average of 3 replicates for each cell line from one of 3 independent experiments. (M) Overexpression of GFP as a control, Cas9-resistant wild-type (wt) HDAC6 and Cas9-resistant catalytically-dead (cd) HDAC6 in tamoxifen (TAM)-inducible Cas9/*HDAC6* gRNA RD line to assess change in cell growth 6 days following TAM-induction. Results shown are the average of 4 replicates from one of 3 independent experiments. (N) Western blots against HDAC6 in ERMS cell lines (RD, 381T and SMS-CTR) and ARMS cell lines (Rh5 and Rh30) transduced with HDAC6 gRNAs and Cas9 6 days post-transduction (top panel); RD and Rh5 cells with TAM-inducible CRISPR-mediated targeted disruption of *HDAC6* (bottom left panel) and in RD TAM-inducible Cas9/*HDAC6* gRNA line overexpressing GFP, wt HDAC6 and cd HDAC6 (bottom right panel) 6 days post-TAM induction. *HDAC6*g = *HDAC6* gRNA. GAPDH was used as a loading control. % depletion relative to the control following normalization to GAPDH as the loading control was quantified by Image J. (O-R) Representative zebrafish ERMS tumors expressing GFP scrambled gRNA control vector (O, Q) and Cas9/*hdac6* gRNA (P, R) over 7 days of growth. (S) Summary of tumor growth. n = 10 for control tumors and n = 8 for double *hdac6* gRNA-targeted ERMS tumors. Each error bar in graphs of L, M and S represents standard deviation. Two-tailed t-test; ** = $p < 0.01$; *** = $p < 0.001$; **** = $p < 0.0001$.

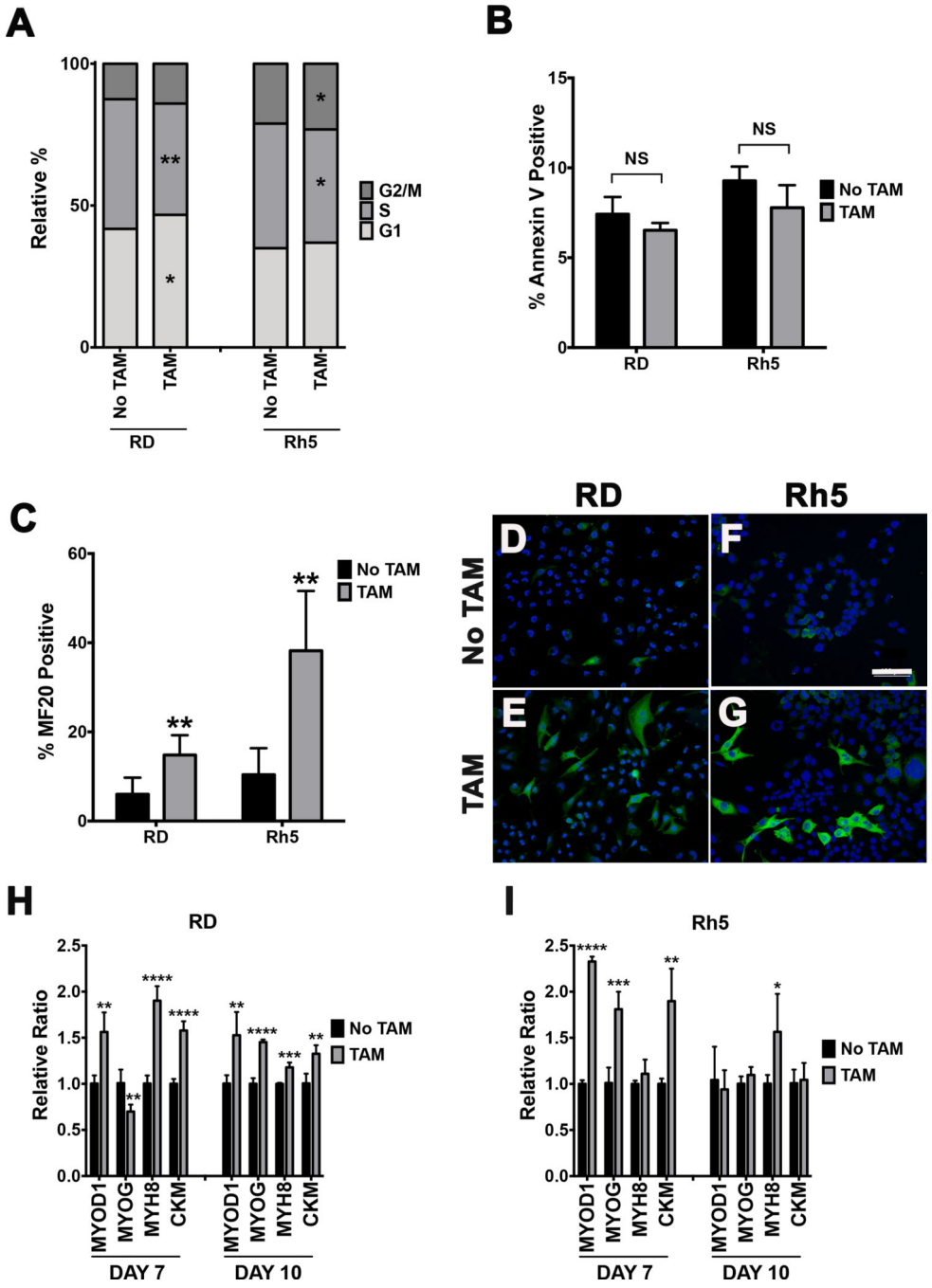

Figure 2. HDAC6 regulates RMS growth by modulating cell cycle progression and tumor cell differentiation.

(A) EdU flow cytometry-based cell cycle analysis of tamoxifen-inducible Cas9-mediated *HDAC6* targeted RD and Rh5 cells day 6 post-tamoxifen treatment. *HDAC6*g = *HDAC6* gRNA. (B) Cell death analysis by Annexin V-based flow cytometry assay in the same RD and Rh5 cell lines 6 days post-tamoxifen treatment. Summary graphs in A-B are results from the average of 3 technical replicates from 1 representative experiment of 3 independent repeats. (C) Quantitation of immunofluorescence (IF) against MF20 in RD and Rh5 cells following 72 hours of serum starvation in 2% horse serum and 7 days post-tamoxifen-

induced CRISPR/Cas9-mediated *HDAC6* targeting. Average of 4 fields at 400X for each condition was shown. (D-G) Representative IF images in RD (D-E) and Rh5 (F-G) cells. Scale bar = 100 microns. (H-I) Quantitative RT-PCR assessing expression of myogenic genes 7 days and 10 days post tamoxifen-induced CRISPR-mediated *HDAC6* gene disruption in RD and Rh5 cells. Results are the average of 4 replicates from one of three independent repeats. Two-tailed t-test was performed for data in A, B, C, H and I; * = $p < 0.05$; ** = $p < 0.01$; *** = $p < 0.001$; **** = $p < 0.0001$.

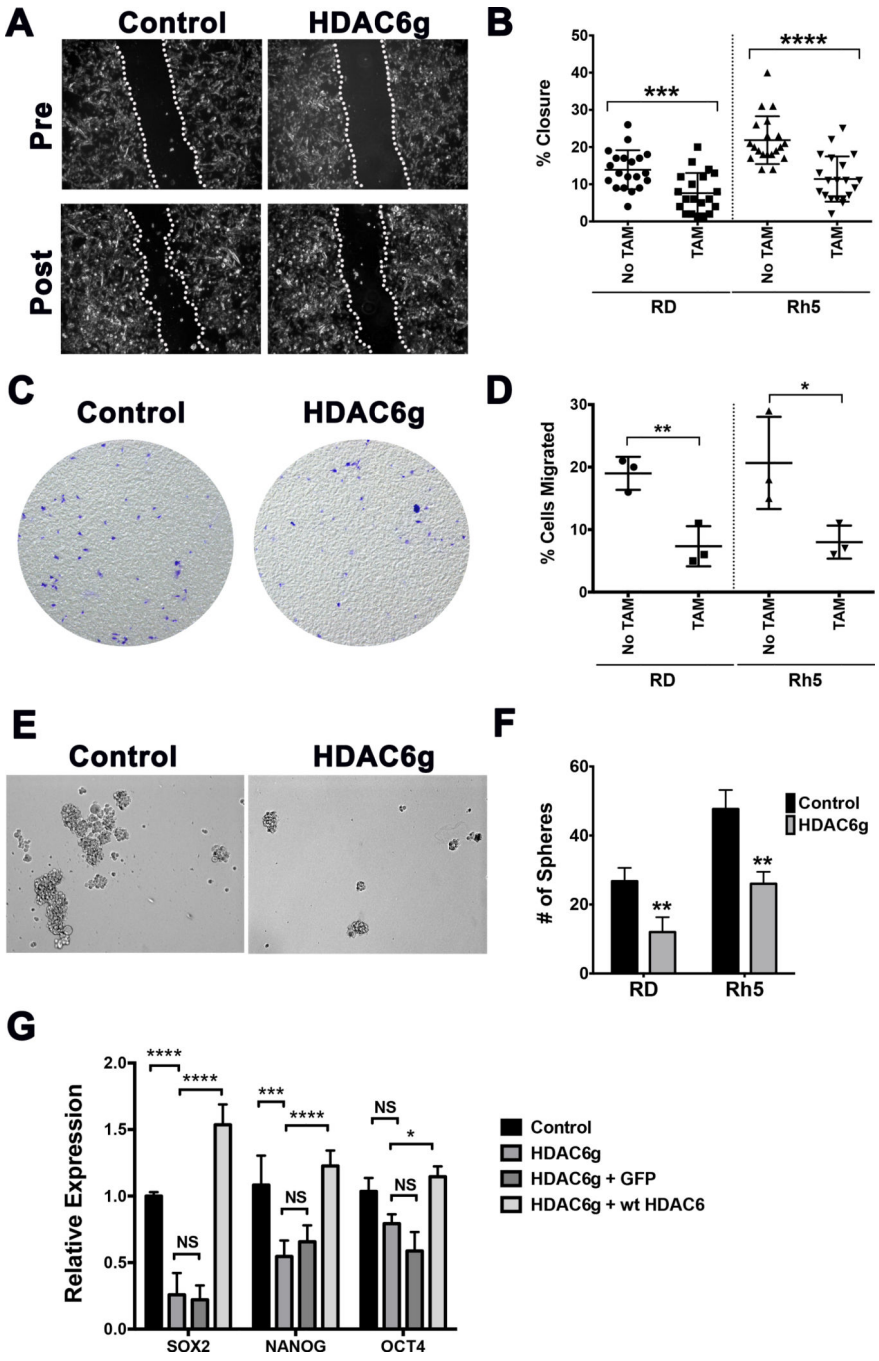

Figure 3. HDAC6 regulates RMS tumor cell migration and self-renewal.

(A) Representative images from a wound healing scratch assay in RD cells with tamoxifen-induced CRISPR/Cas9 *HDAC6* targeting. Post = 16 hours post-scratch. Dashed lines indicate migrating fronts. (B) Summary of scratch assays in RD and Rh5 with tamoxifen-inducible CRISPR/Cas9-mediated *HDAC6* targeting in RD and Rh5. Each datapoint represents a distinct area of the gap. The results shown are from one representative experiment of at least 3 repeats. (C) Representative images from a transwell migration assay. Cells migrated to the bottom chamber were stained with crystal violet at 22 hours post-

seeding in the top chamber. (D) Summary of transwell migration assays in RD and Rh5 with tamoxifen-inducible CRISPR *HDAC6* targeting in RD and Rh5. Each data point represents a replicate well. Results shown are from one of 3 independent experiments. (E) Representative images from a sphere assay in RD cells. (F) Summary of sphere assays in RD and Rh5 cell lines 3 days post-plating. Shown are results of 4 replicates from one of 3 independent experiments. (G) RT-PCR analysis comparing expression levels of stem cell markers in RD sphere cells harboring no TAM control and TAM-induced *HDAC6*-targeting, TAM-induced *HDAC6*-targeting transduced with GFP expression construct and TAM-induced *HDAC6*-targeting transduced with Cas9-resistant wild-type HDAC6 expression construct harvested after 3 days of culturing in stem cell medium. Results were the average of 3 replicates from one of 3 independent experiments. Each error bar in B, D, F and G represents standard deviation. Two-tailed t-test in B, D and F; two-way ANOVA test in G; * = $p < 0.05$; ** = $p < 0.01$; *** = $p < 0.001$; **** = $p < 0.0001$.

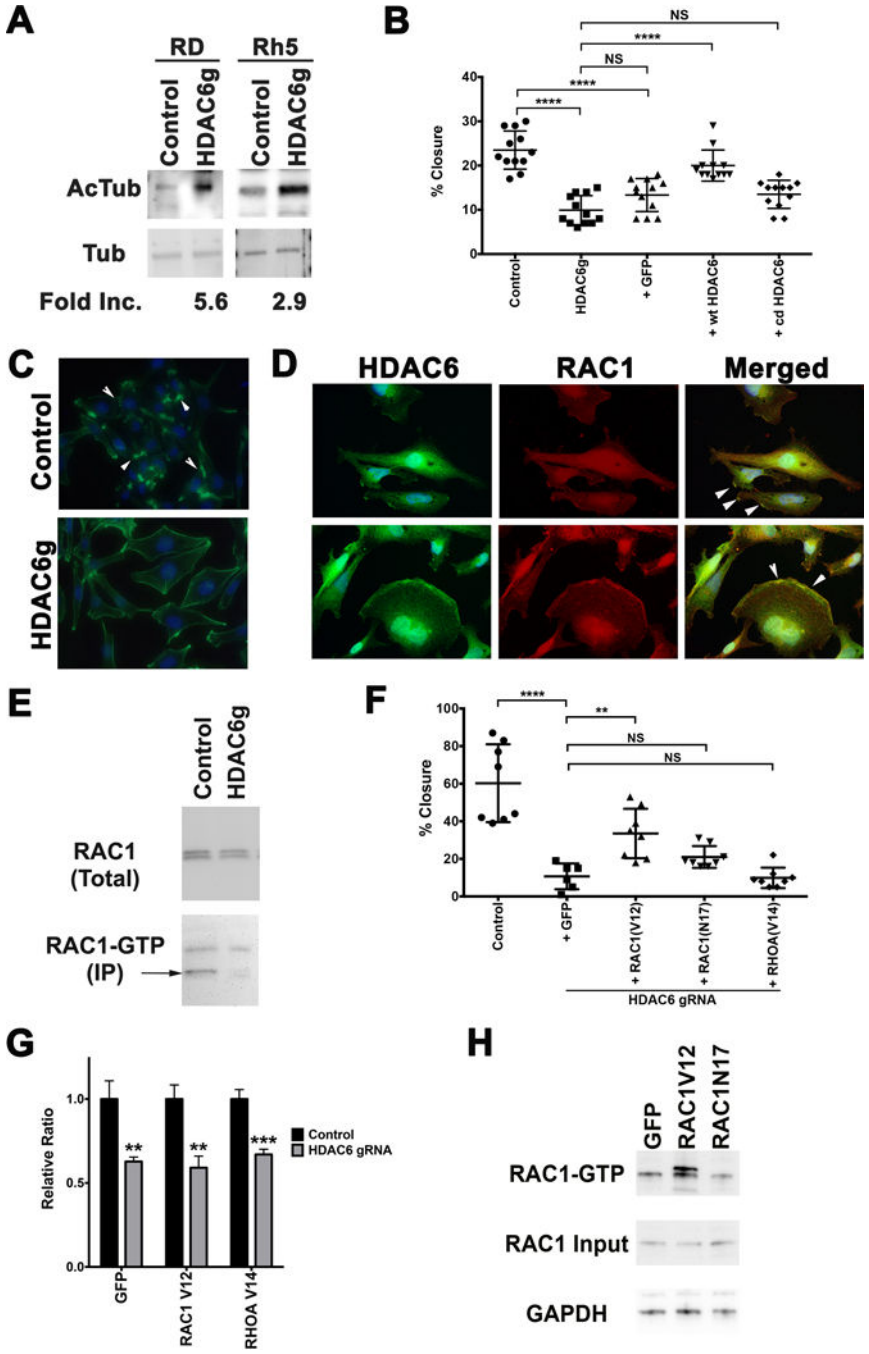

Figure 4. HDAC6 regulates cytoskeletal dynamics to affect RMS cell migration.

(A) Western blots against acetylated alpha-tubulin and alpha-tubulin in RD and Rh 5 cells with tamoxifen-induced CRISPR/Cas9-mediated targeted disruption of *HDAC6* (day 6 post-tamoxifen). Fold increase in the levels of acetylated alpha-tubulin following normalization to the levels of alpha-tubulin was quantified using Image J. (B) Scratch assay assessing effects of adding back Cas9-resistant wild-type (wt) HDAC6 and catalytically-dead (cd) HDAC6 in RD cells with tamoxifen-induced *HDAC6* targeting. Results at 16 hours post-scratch are shown from one representative experiment of at least 3 repeats. (C) Phalloidin staining in

RD cells with no tamoxifen control and tamoxifen-induced *HDAC6* CRISPR targeting following serum starvation and 15-minute EGF (50 ng/mL) treatment at day 6 post-tamoxifen treatment. Arrowheads point to representative areas of membrane ruffles and filopodia formation. Green = phalloidin, Blue = DAPI. (D) Double IF against HDAC6 (green) and RAC1 (red) in RD, showing HDAC6 and RAC1 expression in the regions of membrane ruffles (top panels) and folds (bottom panels), also highlighted by the arrowheads in merged panels. (E) RAC1 GTP pulldown assay in RD cells harboring no tamoxifen control and tamoxifen-induced *HDAC6* CRISPR targeting. (F) Summary of scratch assays assessing the effects of lentiviral overexpression of GFP as a control, RAC1V12, RAC1N17 and RHOAV14 in the presence of tamoxifen-induced CRISPR-mediated targeted disruption of *HDAC6* in RD cells at 16 hours post-scratch following 24 hours of serum starvation and 15 minutes of EGF (50 ng/mL) treatment. (G) Summary of cell growth change by cell counts over 6 days assessing the effects of overexpressing GFP as a control, RAC1V12 and RAC1N17 on cell growth of RD cells with tamoxifen-induced targeted disruption of *HDAC6*. Results were normalized to the no tamoxifen control for each comparison and represent the average of 4 replicates in one of 3 independent experiments. (H) RAC1-GTP pulldown assay in RD cells overexpressing GFP, RAC1V12 and RAC1N17 following 24 hours of serum starvation and 15 minutes of EGF (50 ng/mL) treatment. Each error bar in B, F and G represents standard deviation. Two-tailed t-test in B and G, one-way ANOVA test in F; NS = no significance, $p < 0.05$; ** = $p < 0.01$; *** = $p < 0.001$; **** = $p < 0.0001$.

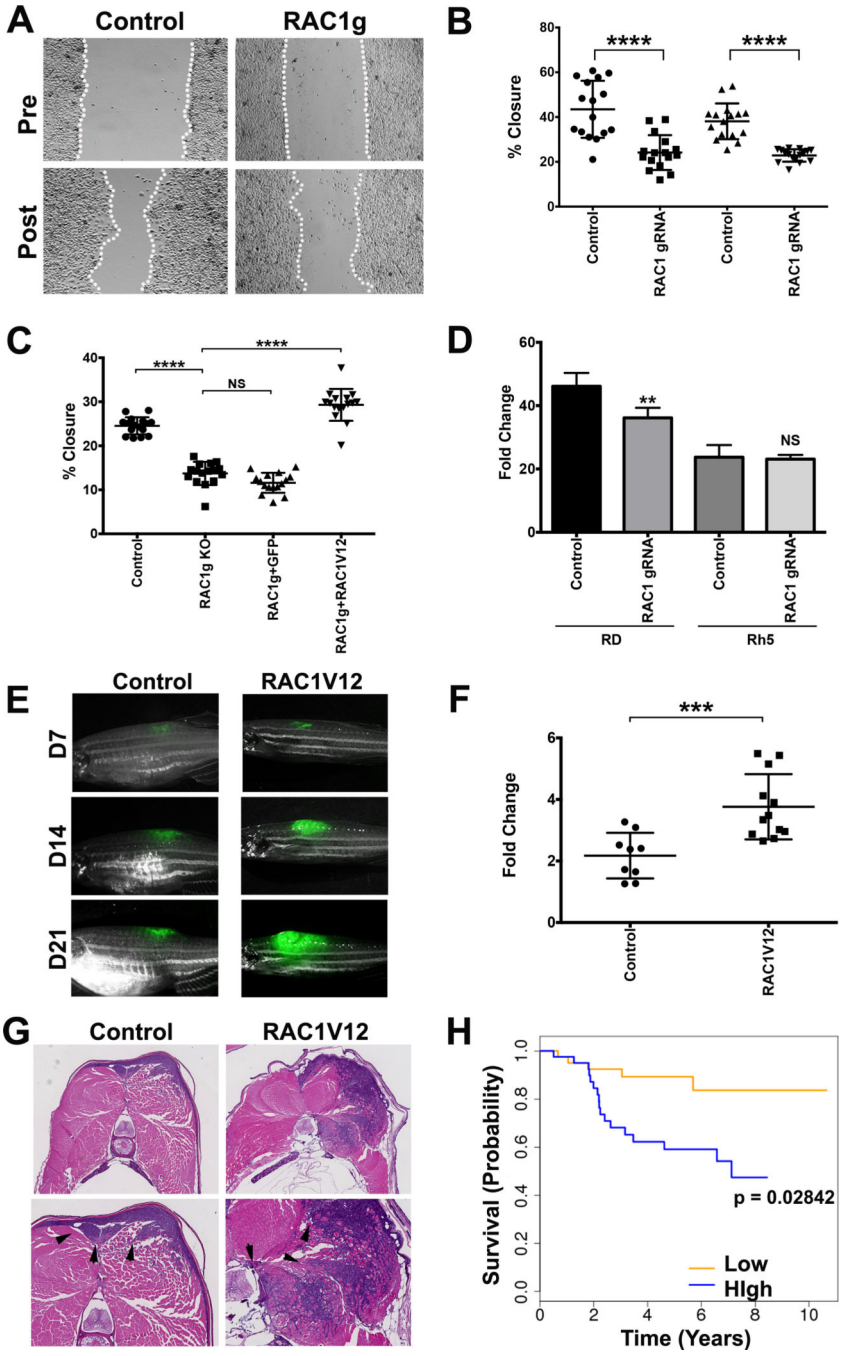

Figure 5. RAC1V12 promotes ERMS tumor growth and invasion.

(A) Representative images of RD cells harboring safe-harbor control targeting and *RAC1* gRNA targeting in a wound healing scratch assay. Dashed lines indicate migrating fronts. (B) Summary of scratch assays in RD and Rh5 cells with targeted disruption of *RAC1*. Each assay was analyzed at 16 hours post-scratch. The results from one of 3 independent replicate experiments are shown. (C) Summary of scratch assays in RD cells transduced with lentivirus expressing safe-habor control gRNA, *RAC1* gRNA, *RAC1* gRNA + GFP, *RAC1* gRNA + RAC1V12 and analyzed at 16 hours post-scratch following plating at the same cell

density at 80–90% confluence. (D) Summary of cell counts in RD and Rh5 cells at 7 days post-plating following lentiviral CRISPR/Cas9-mediated *RAC1* gene disruption (starting cell density = 10,000). (E) Representative images of KRASG12D-induced zebrafish ERMS tumors co-expressing GFP and an empty vector (control) or mutant RAC1V12 at day 7, 14 and 21 post-transplantation. (F) Summary growth volume change for each fish over the first 7 days. n = 8 for control and n = 12 for human RAC1V12-expressing tumors. (G) Representative H&E images of control and RAC1V12 expressing zebrafish ERMS tumors. Lower panels show higher magnification with arrow heads indicating areas of skeletal muscle invasion by tumor cells. (H) Correlation of *RAC1* expression levels with overall survival outcome in RMS patients (63 fusion-negative and 18 fusion-positive) by Kaplan-Meier analysis. Error bars in graphs of B, C, D and F represent standard deviation. Two-tailed t-test in B, D and F. One-way ANOVA with multiple comparisons in C; *** = $p < 0.001$; **** = $p < 0.0001$.

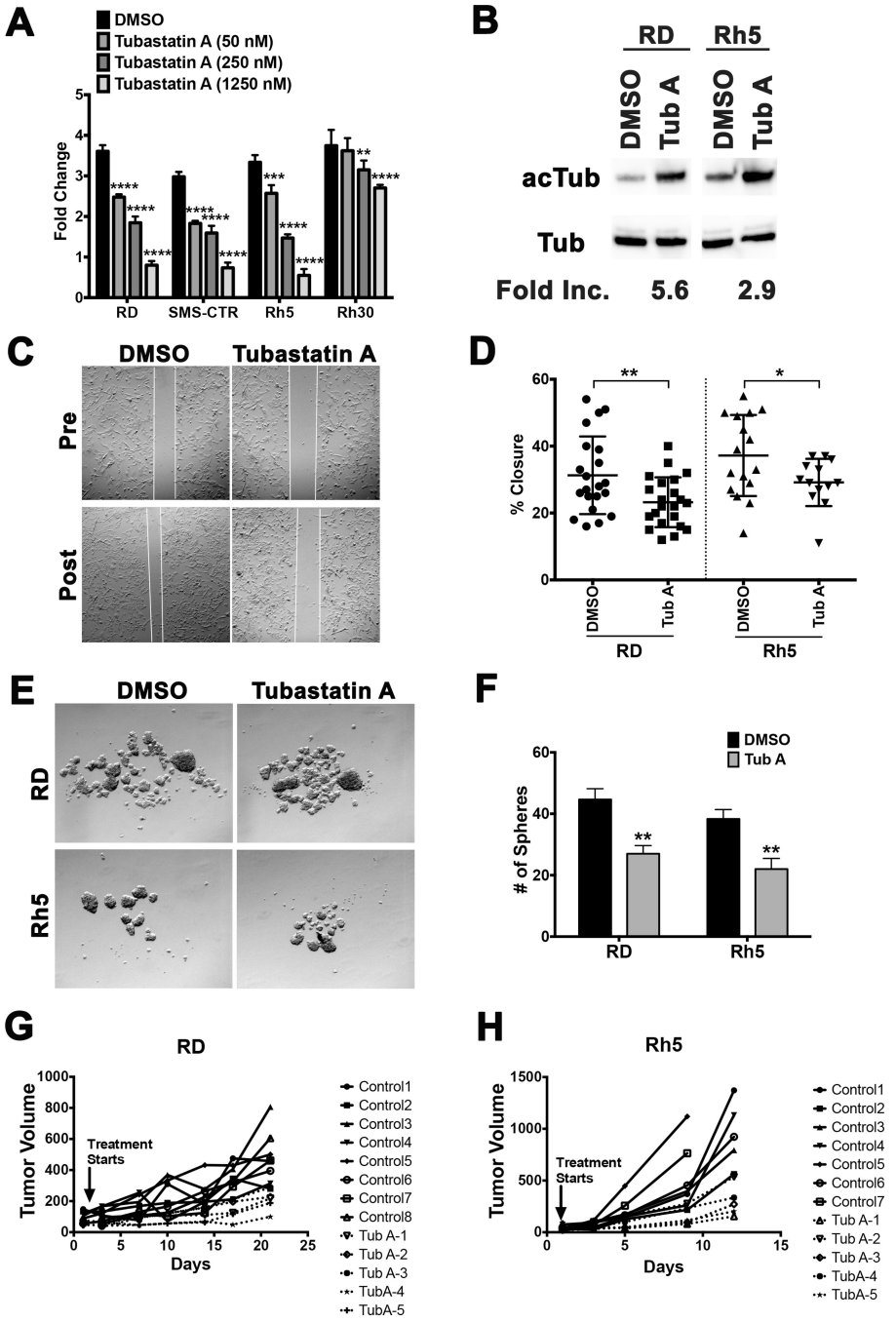

Figure 6. Tubastatin A treatment of RMS cells mimics the HDAC6 loss-of-function phenotypes.

(A) Cell Titer Glo viability assays assessing the dose-dependent effect of tubastatin A on cell growth of RD and Rh5 cells over 5 days. Each dose was done in 4 replicate wells. Results from one representative experiment of at least 3 repeats are shown. (B) Western blots with antibodies against acetylated alpha-tubulin (acTub) and alpha-tubulin (Tub) in RD and Rh5 cells treated with DMSO (vehicle control) or tubastatin A (200 nM) at 24 hours. Fold increase in the levels of acetylated alpha-tubulin following normalization to the levels of alpha-tubulin was quantified using Image J. (C) Representative images from a scratch assay

in RD cells following treatment with DMSO (vehicle) or tubastatin A (200 nM). (D) Summary of scratch assay analysis in RD and Rh5 cells treated with DMSO or tubastatin A (16 hours post-scratch). Results shown are from one representative experiment of 3 repeats. (E) Representative images of sphere assays in RD and Rh5 cells treated with DMSO or tubastatin A (200 nM) for 3 days. (F) Summary of sphere assay analysis in RD and Rh5 cells from one representative experiment of 3 repeats. (G-H) RMS xenografts were established using the RD cell line (G) and Rh5 cell line (H) and treated with tubastatin A (10 mg per kg per mouse, intraperitoneal injections every 3 days for up to 21 days). Treatment for Rh5 xenografts ended early due to many control tumors reaching tumor end point (750 mm^3) per approved animal protocol. Tumor volume change over the treatment period is shown for each tumor-bearing mouse. Each data point represents a mouse. Each error bar in the graphs of A, D and F represents standard deviation. Two-tailed Student's t-test; * = $p < 0.05$; ** = $p < 0.01$; *** = $p < 0.001$; **** = $p < 0.0001$.

Table 1.

Summary of Limiting Dilution Assays

	Experiment 1		Experiment 2		Experiment 3	
Cell No.	**DMSO**	**Tubastatin A**	**DMSO**	**Tubastatin A**	**DMSO**	**Tubastatin A**
10,000	6 of 6	7 of 7	8 of 8	6 of 10	6 of 6	6 of 7
1,000	5 of 6	5 of 10	6 of 10	3 of 10	9 of 10	6 of 10
100	3 of 6	1 of 10	2 of 9	0 of 10	4 of 10	2 of 9
TPC frequency	1350	9045 *	908	8167 *	332	2138 *
95% CI	605–3017	3820–21419	605–3017	3820–21419	161–686	932–4908

* p = 0.001

* p = 2.77e-0

* p = 9.82e-05